



# ISAE

Iranian Society of Automotive Engineers

## International journal of AUTOMOTIVE ENGINEERING

The **International Journal of Automotive Engineering** is recognized as a **Scientific-Research** journal by the Iran Ministry of Science, Research and Technology.

The Journal is published by **Iranian Society of Automotive Engineers (ISAE)** with the collaboration of **Iran University of Science and Technology**.

Contact:  
Dr. Behrooz Mashadi  
Managing Editor  
mashadi@isae.ir

Address:  
Office of the International Journal  
of Automotive Engineering,  
Automotive Research Center, Iran  
University of Science and  
Technology, Tehran, Iran  
Postcode: 1684613114  
P.O. Box:  
Tel. +98 (21) 77240363  
Fax. +98 (21) 77240364  
<http://www.ijae.org>  
[ijae@ijae.org](mailto:ijae@ijae.org)

### EDITOR IN CHIEF:

Shojaeefard M. H. Professor, Iran University of Science and Technology  
Chairman ISAE

### EDITORIAL BOARD:

Daneshjoo K.	Professor, Iran University of Science and Technology
Sohrabortpour S.	Professor, Sharif University of Technology
Hakkak M.	Professor, Tarbiat-Modarres University
Noie Baghban S.H.	Professor, Ferdousi University
Ohadi Hamedani A.	Associate Professor, Amirkabir University of technology
Montazeri-Gh M.	Associate Professor, Iran University of Science and Tech.
Kazemi R.	Associate Professor, Khaje-Nasir University of Tech.
Esfahanian M.	Assistant Professor, Isfahan University of technology

### ADVISORY BOARD:

Crolla D. A.	Emeritus Professor, University of Leeds, UK
Wismans J.	Professor, Chalmers University of Technology, Sweden
Gellinka G.	Professor, Waterloo University, Canada
Ahmadi G.	Professor, Clarkson University, USA
Campinne M.	Professor, Chairman UBIA, Belgium
Hohl G.	Professor, Vice President ÖVK, Austria



# International journal of **AUTOMOTIVE ENGINEERING**

## **Nonlinear Large Deformation Analysis of Rubber Bumpers in Automotive Suspensions**

Sh. Azadi and F. Forouzes

1

## **Evaluation of Effective Parameters on EGR/Blowby Distribution**

P. Bashi Shahabi, H. Niazmand and M. R. Modarres Razavi

10

## **Vehicle's Velocity Time Series Prediction Using Neural Network**

A. Fotouhi, M. Montazeri-Gh and M. Jannatipour

21

## **Effect of injection characteristics on emissions and combustion of a gasoline fuelled partially-premixed compression ignition engine**

A. Nemati, Sh. Khalilarya, S. Jafarmadar, H. Khatamnezhad and V. Fathi

29

## **Dynamical Analysis and Design of Front Engine Accessory Drive System**

B. Mashadi and E. Zakeri

38

## **Performance Analysis of a Variable Geometry Turbocharger Using Mean Line Method**

J. Mahdavinia, A. Keshavarz and M. H. Moshrefi

47

## **Optimized Braking Force Distribution during a Braking-in-Turn Maneuver for Articulated Vehicles**

E. Esmailzadeh, A. Goodarzi and M. Behmadi

56



# Nonlinear Large Deformation Analysis of Rubber Bumpers in Automotive Suspensions

Sh. Azadi<sup>1</sup> and F. Forouzesh<sup>2,\*</sup>

<sup>1</sup> Assistant Professor, Faculty of Mechanical Engineering, K. N. T. University of Technology, P.O. Box 19395-1999, Tehran, Iran. (Email address: azadi@kntu.ac.ir)

<sup>2,\*</sup> Corresponding author, Master of Science, Faculty of Mechanical Engineering, K. N. T. University of Technology, P.O. Box 19395-1999, Tehran, Iran. (Email address: fforouzesh@dena.kntu.ac.ir)

## Abstract

In this article, rubber bumpers of Double - Wishbone suspension system have been modeled and analyzed. The objective of the present work is to predict the performance of these products during deformation, represent an optimum method to design, obtain stiffness characteristic curves and utilize the results in the automotive suspension dynamic analysis. These parts are nonlinear and exhibit large deformation under loading. They have an important role to limit the motion of wheels and absorb energy. In this study, nonlinear FE model using ABAQUS software was used to obtain the bumper load - displacement curve. Then a laboratory test was done on the bumper to get this curve. The comparison between numerical and experimental results shows a good adaptation. A less than 2 percent difference has been observed between them. Thus, we can use this numerical method to simulate bumpers easily and accurately.

**Keywords:** Rubber Bumpers, Automotive Suspension, Nonlinear Analysis, Large Deformation, FE

## 1. INTRODUCTION

Rubber is an engineering material and has isotropic, nonlinear behavior and exhibits large deformation under loading. Many parameters, such as the amplitude of the loading or the temperature, influence its behavior [1]. These materials, because of their recovery and energy absorbing behavior during impact as well as light weight and moldable characteristics, are used extensively in automotive industry. Engine mounts, rubber bushes and rubber stopper bumps applied to suspension systems are a few examples of them [2].

Rubber bumpers are applied to suspension systems to protect against metal to metal contact, limit the motion of wheels, absorb vibrations and decrease the transmissibility of the road irregularities to the vehicle [3].

There are many numerical methods for problem solving, but FEA is the most accurate, versatile and comprehensive method for solving complex design problems such as nonlinear analysis of rubber material parts. FEA of elastomers became a reality for the elastomer component design engineer in the early 1970s with commercial finite element programs such as MARC. Since that time, FEA programs such as ANSYS and ABAQUS have incorporated analyzing

elastomer materials [4]. Due to complex mechanical behavior of elastomers, an appropriate material model is required to analyze rubber components.

Snowdon [5] described the manner in which the internal damping and the dynamic elastic module of rubberlike materials depend upon frequency and temperature and derived a simple general equation from which the transmissibility of any rubber type material may be estimated, provided the frequency dependence of the dynamic shear modulus and the associated damping factor of the material. Hill [6] obtained an exact expression for small radial deformations of bonded cylindrical rubber bush mountings of finite lengths for the applied force. Fourier and Fourier-Bessel series were used for the solution. Garmaroudi. A et.al [7] represented an optimum method to design engine mounts using spring with damping to model these rubber parts by ANSYS.

In this paper rubber bumper of Double - Wishbone suspension system is modeled and analyzed by nonlinear FEM using ABAQUS to obtain load-displacement curve. The bumper used in the present work is made from natural rubber filled with 65 phr carbon black. This type of material is known as hyperelastic. The hyperelastic model and proper strain energy potential are utilized to define the mechanical

properties of the material in software. Then a laboratory test is done to evaluate the simulation results. The comparison between numerical and experimental results shows a good agreement. A less than 2 percent difference has been observed between them.

The purpose of this work is to model rubber bumper instead of using springs in the analysis to observe the effects of geometry and material nonlinearity of these parts to provide real conditions. Also representing an optimum method to design, obtaining stiffness characteristic curves and utilizing the results in the automotive dynamic analysis can be mentioned as some achievements of this study.

## 2. DEFINITION OF ELASROMERIC CHARACTERISTICS

Possessing a nonlinear behavior at high deformation is one of the characteristics of the rubbers. Thus it is necessary to use the theory of large deformations for them. The Green - Lagrange strain tensor is written as follows [8]:

$$\Delta = \frac{1}{2}(C - I) = \frac{1}{2}(F^T \cdot F - I) \quad (1)$$

Where  $\Delta$ ,  $C$  and  $I$  are Green - Lagrange deformation tensor, right Cauchy-Green tensor, and tensor unit, respectively.  $F = \frac{\partial U}{\partial x} + I$  is tensor gradient in which  $U$  is deformation tensor. In the Cartesian coordinates, it will be written in index notation:

$$F_{ij} = \frac{\partial U_i}{\partial x_j} + \delta_{ij} \quad (2)$$

Thus the strain tensor is:

$$\Delta_{ij} = \frac{1}{2} \left( \frac{\partial U_i}{\partial x_j} + \frac{\partial U_j}{\partial x_i} + \sum_{k=1}^3 \frac{\partial U_k}{\partial x_j} \cdot \frac{\partial U_k}{\partial x_i} \right) \quad (3)$$

The expression of this strain tensor takes the geometric nonlinearity of the rubber into account. Strain energy concepts are commonly used to predict rupture of rubbers. The strain energy density can be written as separable functions of a deviatoric component and a volumetric component; i.e.,  $W = W_{dev}(\bar{I}_1, \bar{I}_2) + W_{vol}(J_{el})$  in which  $\bar{I}_i$  is deviatoric strain invariant and  $J_{el}$  is the elastic volume ratio as defined below [9]:

$$J_{el} = \frac{J}{J^{th}} \quad (4)$$

Where  $J$  is the total volume ratio and  $J^{th} = (1 + \varepsilon^{th})^3$  is the thermal volume ratio in which  $\varepsilon^{th}$  denotes the linear thermal expansion strain that is obtained from the temperature and the isotropic thermal expansion coefficient.

The first and second deviatoric strain invariants are:

$$\begin{aligned} \bar{I}_1 &= \bar{\lambda}_1^2 + \bar{\lambda}_2^2 + \bar{\lambda}_3^2 \\ \bar{I}_2 &= \bar{\lambda}_1^{(-2)} + \bar{\lambda}_2^{(-2)} + \bar{\lambda}_3^{(-2)} \end{aligned} \quad (5)$$

Where  $\bar{\lambda}_i = J^{-\frac{1}{3}} \lambda_i$  is deviatoric stretches in which  $\lambda_i = 1 + \varepsilon_i$  denotes the principal stretch ratio, defined as the ratio of stretched length to unstretched length of the edge of an element, and  $\varepsilon_i$  is the corresponding principal extension.

Stress-strain relations are obtained from the strain energy potential. Piolat-Kirchhoff T stress tensor of a homogeneous, isotropic and hyperelastic material is written as follows:

$$T = \frac{\partial W}{\partial \Delta} \quad (6)$$

The mechanical response of a material is defined by choosing a strain energy potential to fit the particular material.

ABAQUS software is one of the powerful commercial programs to model rubber materials with a wide range of strain energy potential forms such as Mooney- Rivlin, Ogden, Yeoh, polynomial form, Neo - Hookean, Marlow, Van der Waals, Arruda - Boyce and etc.

Generally for the hyperelastic material models available in ABAQUS, we can either directly specify material coefficients or provide experimental test data (uniaxial, equibiaxial, volumetric or planar test data) to automatically determine appropriate values of the coefficients by ABAQUS. These material tests are done to get stress-strain curve of the specimens of the material from which the elastomer part is made. Thus this curve depends on part material and is independent of the part geometry. The Mooney - Rivlin model is the most widely used strain energy function due to its simplicity and robustness but it is inadequate in describing the compression mode of deformation [4]. Generally, when data from multiple experimental tests are available the Ogden and Van der Waals forms are

more accurate in fitting experimental results. If limited test data are available, the Arruda - Boyce, Yeoh, or reduced polynomial forms provide reasonable behavior. In the present paper since the uniaxial tension test data was just available for the material used, the Yeoh form was selected because this model has been demonstrated to fit various modes of deformation using data from a uniaxial tension test only [4]. The strain energy potential for this form is [9]:

$$\begin{aligned} \text{Yeoh form:} \\ W = C_{10}(\bar{I}_1 - 3) + C_{20}(\bar{I}_1 - 3)^2 + C_{30}(\bar{I}_1 - 3)^3 \\ + \frac{1}{D_1}(J^{el} - 1)^2 + \frac{1}{D_2}(J^{el} - 1)^4 + \frac{1}{D_3}(J^{el} - 1)^6 \end{aligned} \quad (7)$$

Where  $C_{i0}$  and  $D_i$  are material parameters.

The properties of rubber type materials can vary significantly from one batch to another; therefore, if data are used from several experiments, all of the experiments should be performed on specimens taken from the same batch of material.

### 3. NONLINEAR ANALYSIS WITH LARGE DEFORMATION OF RUBBER BUMPER

#### 3.1. Nonlinear Finite Element Analysis of rubber bumper

Since rubber materials are nonlinear and exhibit large deformation under loading, in this study nonlinear finite element analysis by ABAQUS, a robust computer program to model elastomers with such complex characteristics, has been used to investigate the static deflection and load-displacement curve of the rubber bumper.

Figure (1) shows the rubber bumper and Double - wishbone suspension system in which it is applied. The bumper is connected to the lower control arm as shown in figure (1).

The 3D - geometry and 2D - drawing of the rubber bumper modeled in CATIA is depicted in figure (2).

The bumper used in the present work is made from natural rubber filled with 65 phr carbon black. The stress-strain curve of the material of this bumper from a uniaxial tension test is shown in figure (3). The stress-strain behavior of rubbers is elastic but highly nonlinear. This type of material behavior is known as hyperelasticity. A convenient way of defining a hyperelastic material is to supply ABAQUS with material test data by specifying strain energy potential.

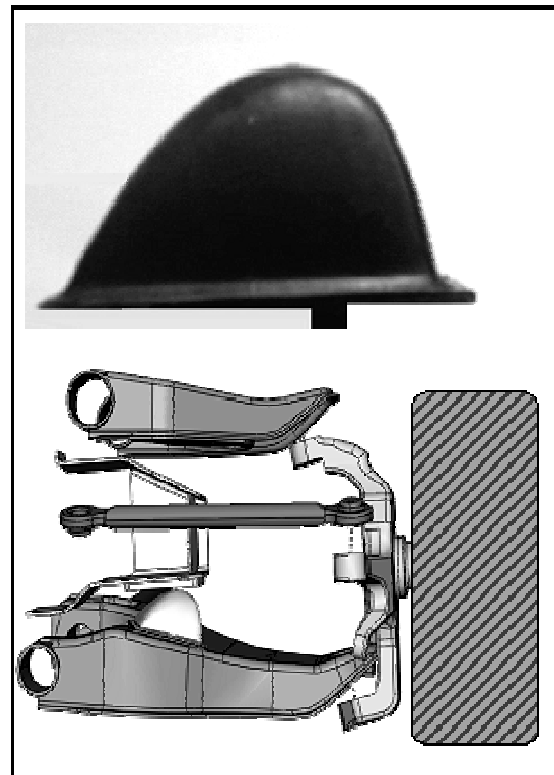


Fig. 1. rubber bumper and Double-wishbone suspension

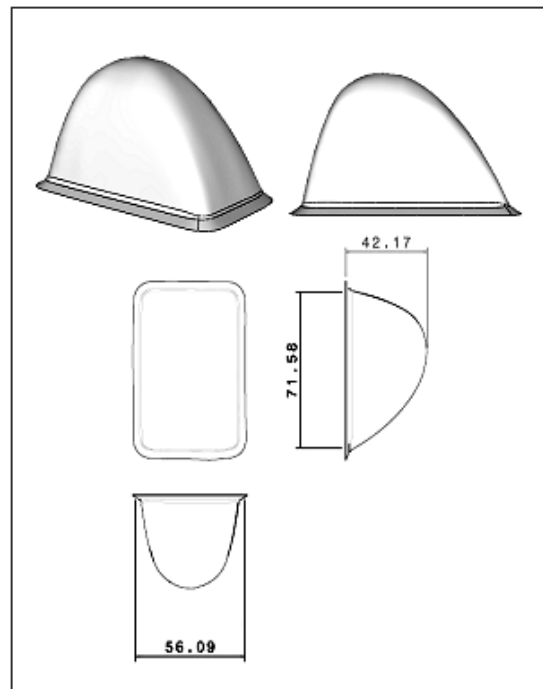
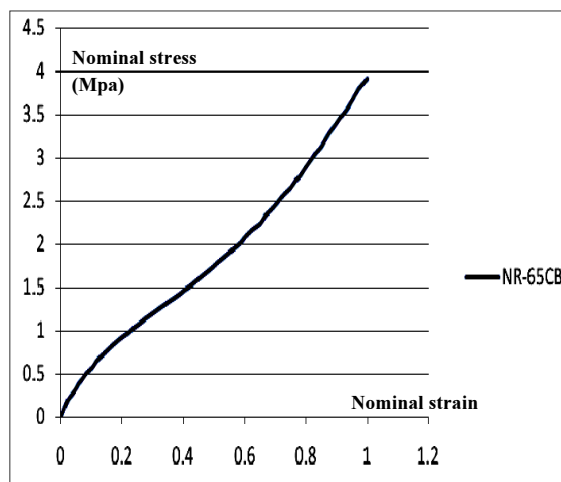


Fig. 2. the 3D-geometry and 2D-drawing of rubber bumper



**Fig. 3.** The stress-strain curve of the material of the bumper from a uniaxial tension test

In the present work since the uniaxial tension test data was just available for the material used, the Yeoh form was selected. Table (1) presents the material parameters of Yeoh form,  $C_{i0}$  and  $D_i$ , estimated by ABAQUS according to the input material test data shown in figure (3).

To check the accuracy of the selected strain energy potential form, the stress-strain curve of the material depicted in figure (3) has been compared with the estimated curve by ABAQUS using Yeoh form in figure (4).

Figure (4) shows a little error between two curves, thus Yeoh form is appropriate to model the characteristics of the bumper material. In addition to the provision of the material test data to determine a hyperelastic material, density and Poisson's ratio are also required. Density and Poisson's ratio of the used

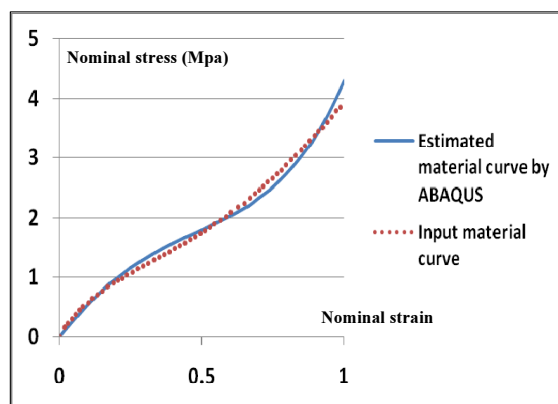


**Fig. 4.** The comparison between estimated material curve by ABAQUS using Yeoh form and Input material data

**Table 1.** the material parameters of Yeoh form estimated by ABAQUS according to the input material test data

$C_{10}$	1.00532	$D_1$	1.99 e-3
$C_{20}$	-0.2112	$D_2$	0
$C_{30}$	8.89 e-2	$D_3$	0

rubber are 1.2 g/ml and 0.49 respectively. Most elastomers have very little compressibility. In cases where the material is highly confined, the compressibility must be modeled correctly to obtain accurate results but in applications where the material is not highly confined, the degree of compressibility is typically not crucial. The relative compressibility of a material can be modeled by the ratio of its initial bulk modulus,  $K_0$ , to its initial shear modulus,  $\mu_0$ . This ratio can also be expressed in terms of Poisson's ratio ( $\nu$ ) [9]:

$$\nu = \frac{3K_0 / \mu_0 - 2}{6K_0 / \mu_0 + 2} \quad (8)$$

If no value is given for the material compressibility in the hyperelastic model, by default ABAQUS assumes  $K_0 / \mu_0 = 2\nu$ , corresponding to Poisson's ratio of 0.475. Since the Poisson's ratio of typical unfilled elastomers is 0.4995 - 0.4995 and filled elastomers is 0.490 - 0.497, this default provides much more compressibility than is available in most elastomers. Temperature effects and the visco-elastic nature of this elastomer are eliminated due to static analysis. The assembly used in ABAQUS to FEA of the rubber bumper has been shown in figure (5). By applying the force - time curve to the flat rigid part, it moves toward the bumper and applies this force to it. Rigid constraint was prescribed to the flat moving part. Also a clamped boundary condition was applied to the bottom surface of the bumper.

Many engineering problems involve contact between two or more components. In these problems a force normal to the contacting surfaces acts on the two

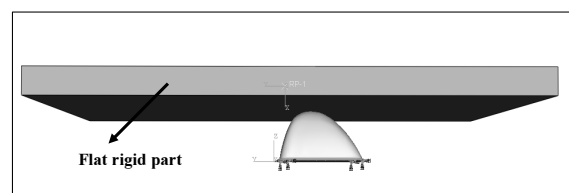


**Fig. 5.** The assembly used to FEA of the rubber bumper



bodies when they touch each other. The general aim of contact simulations is to identify the areas on the surfaces that are in contact and to calculate the contact pressures generated. In a finite element analysis contact conditions are a special class of discontinuous constraint, allowing forces to be transmitted from one part of the model to another. The constraint is discontinuous because it is applied only when the two surfaces are in contact. When the two surfaces separate, no constraint is applied. The analysis has to be able to detect when two surfaces are in contact and apply the contact constraints accordingly. Similarly, the analysis must be able to detect when two surfaces separate and remove the contact constraints. A contact simulation using contact pairs is defined by specifying surface definitions for the bodies that could potentially be in contact and the mechanical and thermal contact property models, such as the pressure-overclosure relationship, the friction coefficient, or the contact conduction coefficient [9]. In this work a surface to surface contact was used to model the contact interaction between bumper surface and flat rigid part surface.

Self-contact is typically the result of large deformation in a model. It is often difficult to predict which regions will be involved in the contact or how they will move relative to each other. Self - contact was used for bumper exterior surface to define the interaction of this surface with itself.

In FEA some factors such as type, shape and size of elements must be considered to have an effective mesh. Because the accuracy of results depends on the accuracy of elements selected. In nonlinear FEA, lower-order elements are often preferred over higher elements, because of reasonable accuracy at reduced cost and their robustness for large deformation analysis. So using a linear element is preferred over quadratic and cubic elements. In nonlinear FEA such as rubber analysis, it is well known that the linear 3-node triangle and 4-node tetrahedron can give incorrect results because they are too stiff. When using lower-order elements, 4-node quadrilaterals and 8-node brick elements perform significantly better than triangle and tetrahedron elements [4]. Figure (6) illustrates the force-displacement curve of the top point of bumper obtained during a static analysis using tetrahedron and brick elements. It is observed that tetrahedron elements curve is stiffer than brick elements curve.

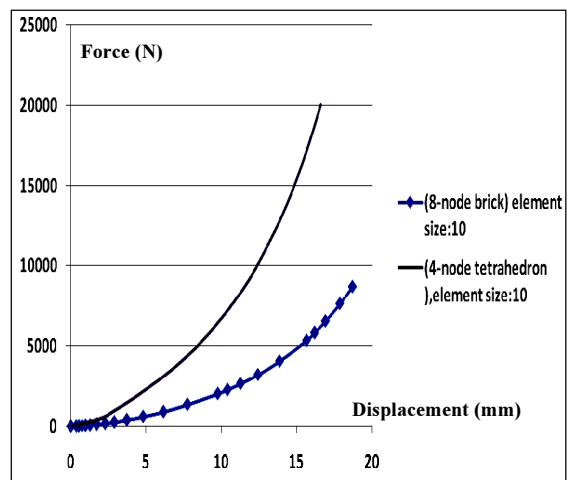


Fig. 6. The force-displacement curve of the top point of bumper using tetrahedron and brick elements

An accurate shape element must satisfy the following conditions [10]:

$$15^{\circ} \leq \text{The corner angle of element} \leq 165^{\circ} \quad (9)$$

$$\text{aspect ratio} \leq 5$$

Where the aspect ratio of an element is the ratio of its longer dimension to its shorter dimension. The displacement and stress convergency curves of some bumper nodes were obtained for different element sizes to select the best one. In order to check the convergency, both coarse and fine elements were used and the best one was selected after the observation of convergency.

Solid elements (8-node first-order brick, hybrid, reduced integration with hourglass control elements) were used for rubber bumper according to important points mentioned above. Figure (7) shows typical finite element mesh of this bumper.

Since flat moving part has rigid constraint, the type of

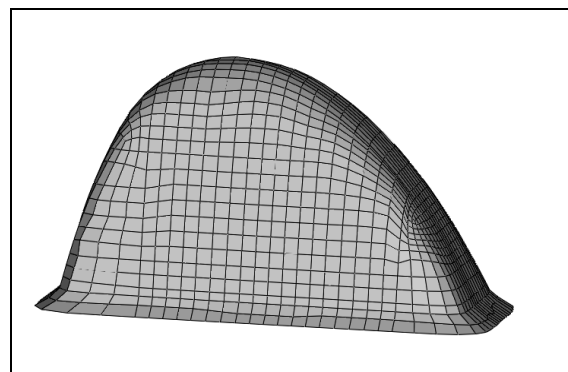


Fig. 7. typical finite element mesh of the bumper

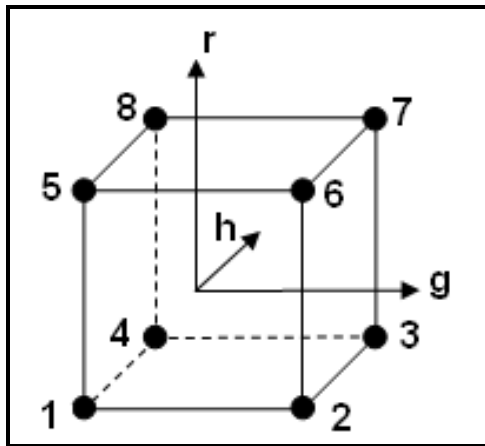


Fig. 8. A first-order brick element

elements isn't important because they won't take into account in the calculations. The interpolation function for first-order brick element is as follows:

$$\phi = \sum_{i=1}^8 N_i(g,h,r) \phi_i \quad (10)$$

$$N_i = \frac{1}{8}(1 + g_i g)(1 + h_i h)(1 + r_i r)$$

Where  $g$ ,  $h$  and  $r$  are element coordinates shown in figure (8),  $N_i$  is shape function and  $\phi_i$  is nodal value. The FE final deformation of the bumper at the maximum force value and the force - displacement curve of the top point of that are presented in figure (9).

### 3.2. Experimental Test and Verifying the FE Results

A laboratory test was done to verify the FE result of bumper load - displacement curve. The compression test of bumper was done using an Instron 1115. Rubber bumper was set between a moving part and a load cell as shown in figure (10).

The speed of moving part was 10 mm/min. The force, applied to the bumper by the moving part, was drawn versus the displacement of the top point of bumper by computer to get load - displacement curve. Since the stress strain function stabilizes after between 3 and 20 repetitions for most elastomers, the bumper has been tested 5 times to obtain a stable curve. Figure (11) shows the results of these five loading cycles. Also the displacement values of the bumper top point

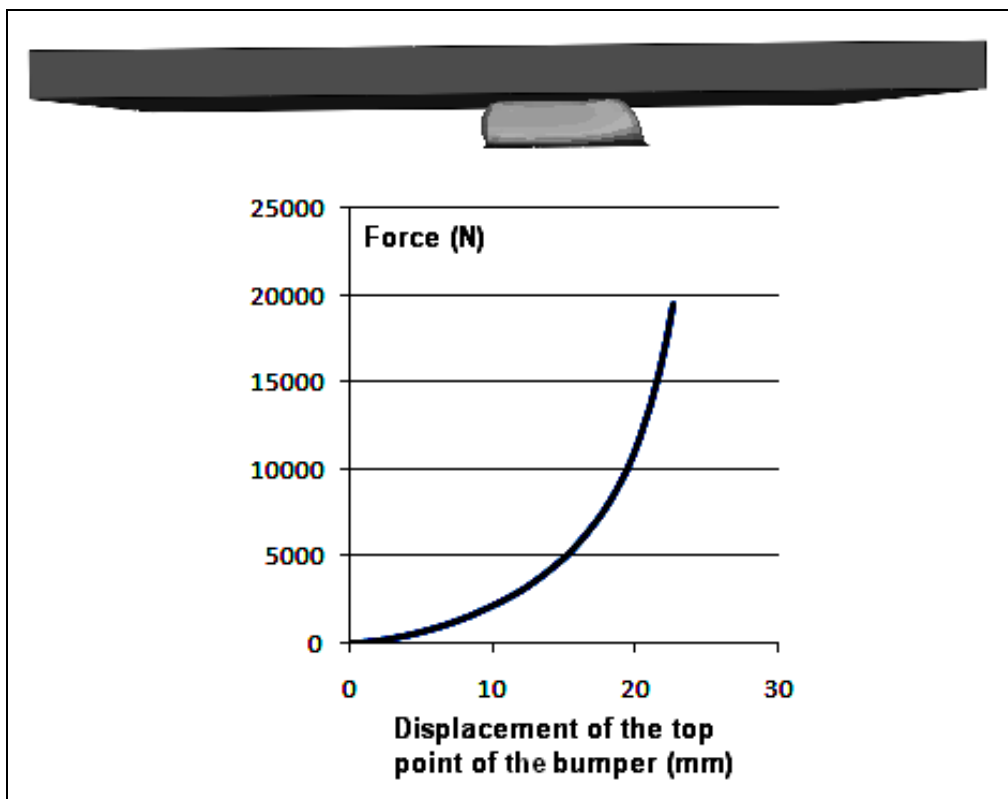


Fig. 9. The force-displacement curve of the top point of the bumper and FE final deformation of that at the maximum value of the force applied

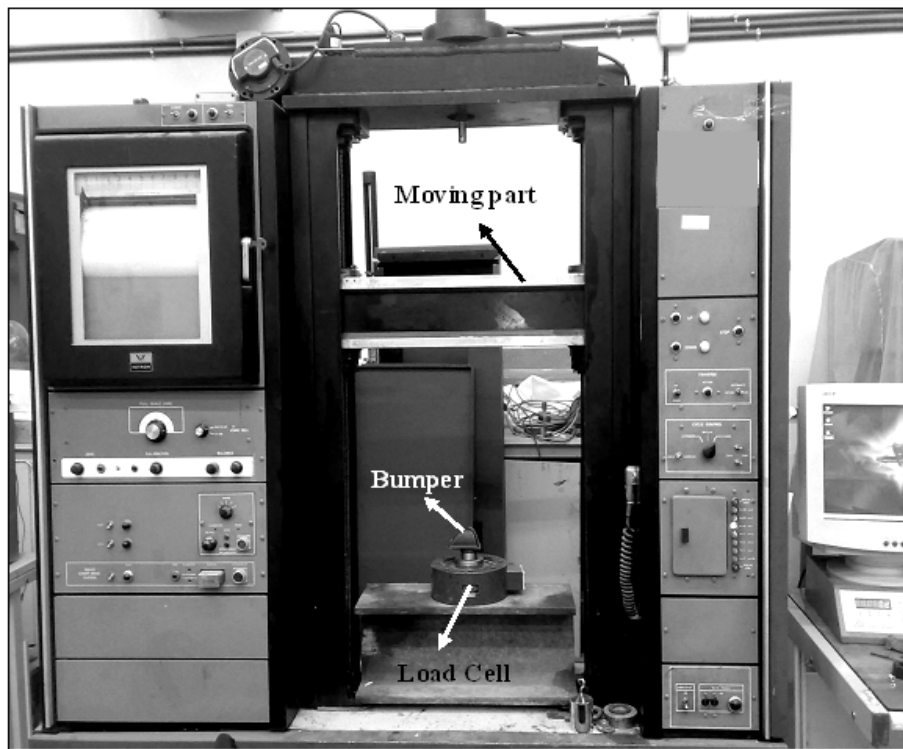


Fig. 10. Instron 1115 for the compression test of the bumper

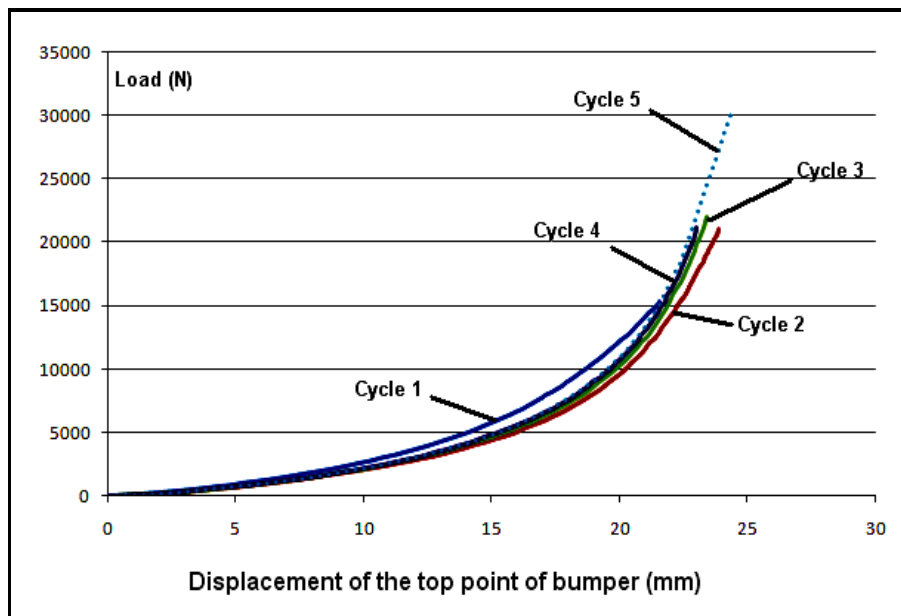


Fig. 11. Load - displacement curves of the bumper corresponding to the first 5 loading cycles at its top point

at 4 arbitrary force values of these cycles have been given in Table (2).

Since the difference between 4<sup>th</sup> cycle and 5<sup>th</sup> cycle is less than 0.8 %, 5<sup>th</sup> cycle was selected as bumper load - displacement curve. The comparison between

numerical and experimental load -displacement curve shows a good agreement. A less than 2 percent difference has been observed between them. This comparison is shown in Figure (12). Figure (13) shows experimental final deformation of the bumper

**Table 2.** experimental displacement values of the bumper top point at several arbitrary force values of the first five loading cycles

Force (N)	Displacement (mm)				
	Cycle1	Cycle2	Cycle3	Cycle4	Cycle5
1500	6.98	8.27	8.17	8.06	8
2500	9.65	11.29	11	10.9	10.82
5000	14.01	15.87	15.50	15.31	15.23
7000	16.27	18.09	17.72	17.48	17.42

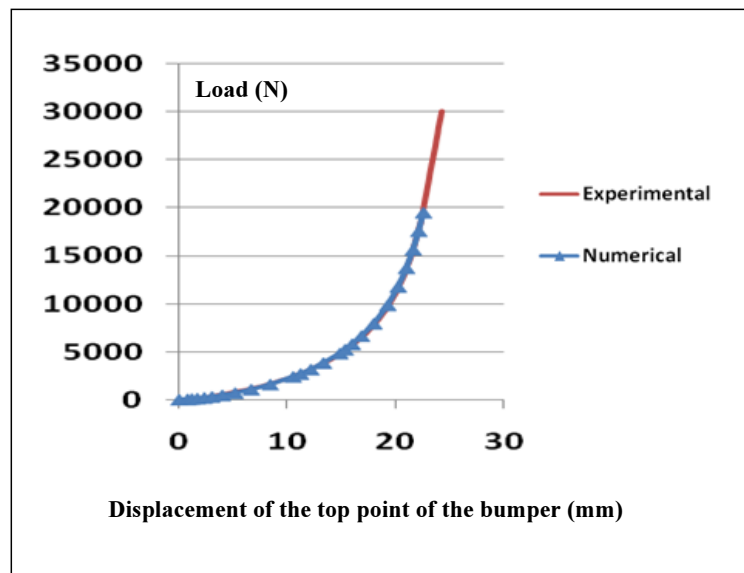


**Fig. 12.** The comparison between numerical and experimental load-displacement curves

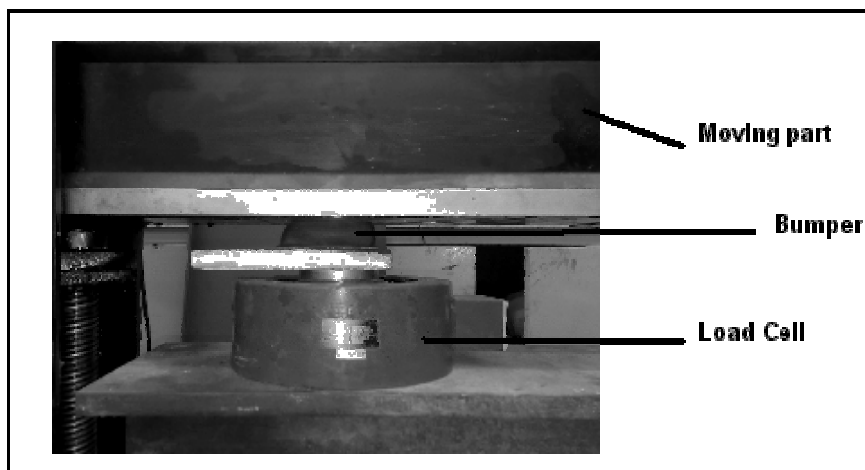


**Fig. 13.** experimental final deformation of the bumper at the maximum value of the used force

at the maximum value of the force applied.

#### 4. CONCLUSIONS

In this paper rubber bumper performance of double-wishbone suspension was considered numerically and experimentally. The nonlinear finite element method by using ABAQUS was used to analyze bumper statically and obtain its load - displacement curve. Rubber bumper was modeled by hyperelastic material model using uniaxial nominal stress-strain data. Because 4-node tetrahedron elements are too stiff and result in incorrect results, 8-node linear brick and hybrid elements were utilized for FE modeling of the bumper. Then a laboratory test was done on the bumper to verify the FE results by its resultant load-displacement curve. The comparison between numerical and experimental characteristic curves of the bumper shows a good adaptation. A less than 2 percent difference has been observed between them. Thus the presented nonlinear FEA can be used to model rubber parts with any shape and material and FE results can be utilized as an input in the automotive dynamic analysis programs such as ADAMS.

#### REFERENCES

- [1] Jezequel, L. Time Model of Rubber Deformation, Journal of Engineering Materials and Technology, 2001, vol. 123, 36-44.
- [2] Uhm, S. W., Yeo, T., Nonlinear Finite Element Analysis Of Rubber Bush With Large Form Factor, Science and Technology, 2003, vol. 1, 320-326.
- [3] Ambrósio, J. and Verissimo, P. Sensitivity of a vehicle ride to the suspension bushing characteristics. Mechanical Science and Technology, 2009, vol. 23, 1075-1082.
- [4] Gent, A. N. Engineering With Rubber: How to design Rubber Components 2nd edition. Hanser, 2001.
- [5] Snowdon, J.C. Rubberlike materials, their internal damping and roll in vibration isolation. Journal of Sound and vibration, 1965, vol. 2, 175-193.
- [6] HILL, J.M. Radical deflections of rubber bush mountings of finite lengths. Journal of IJES, vol. 13, 407-422.
- [7] Garmaroudi, A.M., Azadi, Sh., optimum design

of engine mounts, M.Sc thesis, K.N.Toosi univ. of Tech, 2002,

- [8] Guen, J. Le., Thouverez, F., Demoulin, G., and Jezequel, L. Time Model of Rubber Deformation. Journal of Engineering Materials and Technology, 2001, vol. 123, 36-44.
- [9] ABAQUS analysis user's manual, version 6.7, SIMULIA, 2007.
- [10] Shariyat, M. Automotive Body: Design and analysis. K.N.Toosi univ. of Tech, 2009 (in Persian)

#### NOMENCLATURE

<b>C</b>	right Cauchy-Green tensor
<b>F</b>	tensor gradient
<i>g</i>	element coordinate
<i>h</i>	element coordinate
<b>I</b>	tensor unit
$\bar{I}_i$	deviatoric strain invariant
<i>J</i>	total volume ratio
$J_{el}$	elastic volume ratio
$J_{th}$	thermal volume ratio
$K_0$	initial bulk modulus
$N_i$	shape function
<i>r</i>	element coordinate
<b>T</b>	Pirolat-Kirchhoff stress
<b>U</b>	deformation tensor
<i>W</i>	strain energy density
$\Delta$	Green-Lagrange deformation tensor
$\varepsilon_i$	principal extension
$\varepsilon^{th}$	linear thermal expansion strain
$\phi_i$	nodal value
$\lambda_i$	principal stretch ratio
$\bar{\lambda}_i$	deviatoric stretch
$\mu_0$	initial shear modulus
$\nu$	Poisson's ratio